Six-state algebraic close-coupling calculation of positron-hydrogen scattering at low energies

T. T. Gien
Department of Physics, Memorial University of Newfoundland, St. John's, Newfoundland, Canada A1B 3X7
(Received 11 October 1994; revised manuscript received 17 March 1995)

We did the Harris-Nesbet algebraic close-coupling calculation for positron-hydrogen scattering at low energies with the $(1s,2s)$H-$(1s,2s)$Ps, $(1s,2s,2p)$H-$(1s,2s)$Ps, and $(1s,2s,2p)$H-$(1s,2s,2p)$Ps coupling schemes. Cross sections of elastic scattering, positronium formation, and Ps$(1s)$-p elastic scattering were obtained for $L=0,1,2,3,4,5,6$ partial waves. The integrated cross sections for the relevant processes were then estimated. We compared our six-state close-coupling results with the ones calculated by solving the Lippmann-Schwinger coupled equations in momentum space. Many special features were seen in these cross sections.

PACS number(s): 34.80.−i

INTRODUCTION

In the last decade, the atomic collision physics community has been interested a great deal in positron collisions with atomic targets above the positronium (Ps) formation threshold [1]. The revitalization of this interest is perhaps due to the fact that experimental data for some positronium formation processes have now become available, and experimental research activities on positron collision with atomic targets have been vigorously pursued in laboratories worldwide during recent years [2]. Especially, some experimental data for positron collisions with atomic hydrogen have also appeared in the literature just during the last two years or so [3,4].

On the theoretical side, the calculation of positron scattering from atomic targets is much more difficult than the one for electron scattering. This difficulty arises from the fact that for a realistic calculation, one has to consider the positronium formation channels in the positron case, and dealing with a collision system that gets involved with two different systems of coordinates (depending on whether one is within a hydrogen scattering channel or within a positronium formation channel) is not a simple matter. To carry out their task of analytical reduction of formulas, theorists usually had to transform these two different sets of coordinate variables to the ones that they could use to factorize their reduced formulas. This difficulty may also be the reason for the few detailed theoretical calculations of Ps formation cross sections in the literature.

For positron collisions with hydrogen at energies above the positronium formation threshold, there had been some earlier calculation of positronium formation cross sections using the Kohn variational method [5,6]. However, the calculation up to this point, to our knowledge, had been restricted to only a few lowest partial waves ($L=0$, 1, and 2). In recent years, a few theoretical groups [7–11] have attempted to obtain cross sections for positronium formation and positron scattering from hydrogen with the close-coupling approximation. The number of target states that they included in the close-coupling expansion varied from one calculation to another. Except for the work by Higgins and Burke [10], who employed the R-matrix technique for the calculation, the remaining groups solved the coupled Lippmann-Schwinger equations in momentum space. Unfortunately, the results obtained by these different groups for the same coupling scheme were at times conflicting [7–9,11], even when exactly the same numerical method was used. In the method of solving the Lippmann-Schwinger equations in momentum space, the calculation had to resort to the discretization of the integrals of the coupled equations. This discretization was used to transform the analytic coupled equations to a matrix equation, which could then be solved by known procedures [7,8]. For the nodal points close to the poles of the kernel functions, accurate results of calculation would seem to be difficult to obtain, if care had not been taken to handle the calculation at these nodal points. We suspect that a slightly improper handling of the calculation near the poles may lead to inaccurate or even erroneous results, and this might be the source of the discrepancy that at times exists among results calculated by these various research groups. Thus, it is very much desirable to obtain these close-coupling cross sections by a completely different numerical method for comparison.

In recent years, Liu and Gien [12] and Gien and Liu [13] used the Harris-Nesbet method [14,15] to also carry out the close-coupling calculation for positron-hydrogen scatterings. This algebraic method of approach had been proposed and developed earlier by Harris [14] and Nesbet [15]. It had been successfully considered by Seiler, Oberoi, and Callaway [16] for electron (and positron) scattering below the positronium formation threshold and by Wakid and Labahn [17] and Wakid [18] for positron scattering and positronium formation. Wakid and Labahn [17], however, had done the calculation for S-wave scattering only.

Our Harris-Nesbet algebraic calculations [12,13,19,20] for close-coupling approximation indicated that the method can handle the positronium formation channel well. It can also provide reliable and accurate results for cross sections, especially at low energies. Indeed, the method supplies many self-consistency checks for the reliability of the results of calculation, such as the agreement between the Kohn and inverse Kohn cross sections, the stability of the results of calculation with a change of the values of the stability parameters, and the stability of

the results of calculation with a change of the number of bound basis functions. Within the method, some criterion could also be set to select the more accurate value between the Kohn and inverse Kohn ones [15]. Contrary to popular belief, the Harris-Nesbet method is furthermore anomaly-free [15]. The effect of the singularity near the eigenvalues of the bound basis functions usually does not materialize in the calculation of the reactance matrices. The possibility for producing pseudoresonances in the calculation might not become a matter of concern, if proper care is taken to eliminate them. In more difficult cases (concerning the zeros between poles of M_{00} and M_{11}), Nesbet and Harris also proposed various improved procedures to overcome the anomaly [15,21].

In this work, we employed the Harris-Nesbet method to carry out an extensive calculation of positronium formation, elastic e-H scattering and elastic Ps($1s$)-p scattering cross sections, with the consideration of a more enlarged six-state coupling scheme ($1s,2s,2p$)H-($1s,2s,2p$)Ps. These states are the first six lowest "actual" states of the positron-hydrogen collision system. The calculation was done for the lowest seven partial waves ($L=0$, 1, 2, 3, 4, 5, and 6). To our knowledge, the Harris-Nesbet method has never been used to do high partial-wave ($L=6$) close-coupling calculations for a coupling scheme that contains excited Ps states. Note that within the Harris-Nesbet method, the inclusion of excited Ps states to the coupling scheme in the case of a high partial wave required the development of an additional set of general formulas. As was mentioned above, results obtained by different research groups for this six-state coupling scheme [7–9,11] were conflicting. Our calculation with the Harris-Nesbet method for this coupling scheme can, therefore, also be used to resolve this controversy. For comparison, we also carried out our Harris-Nesbet calculation with the ($1s,2s$)H-($1s,2p$)Ps and ($1s,2s,2p$)H-($1s,2s$)Ps coupling schemes. Since calculations employing variational techniques have been known to be reliable at low scattering energies, we limited our calculation in this work to scattering energies below the first excitation threshold of H, where conflicting results obtained by other research groups seemed to exist.

The plan of this paper is as follows. For the sake of clarity, we briefly review the basic formalism of the Nesbet-Harris method in Sec. I. We also briefly describe in Sec. II how to transform the relevant formulas to expressions that can be ready for use in subsequent numerical calculations. In this section, we also describe the numerical work that we carried out for this calculation. The purpose of this section is to help clarify our subsequent calculation and to expose the effort that we had invested in this calculation in order to achieve these results. In Sec. III, we present the results of our calculation with discussion. Finally, in the Conclusion section, we draw some useful conclusions from this work and briefly mention some subsequent works that we plan to carry out within our project of algebraic close-coupling calculation.

I. FORMALISM

The Hamiltonian of the positron-hydrogen collision system is either

$$H=-\frac{\hbar^2}{2m}\nabla_{r_1}^2-\frac{\hbar^2}{2m}\nabla_{r_2}^2-\frac{e^2}{r_1}+\frac{e^2}{r_2}-\frac{e^2}{|\vec{r}_1-\vec{r}_2|} \quad (1a)$$

or

$$H=-\frac{\hbar^2}{m}\nabla_{\rho}^2-\frac{\hbar^2}{4m}\nabla_R^2-\frac{e^2}{\rho}+\frac{e^2}{\left|\vec{R}-\frac{\vec{\rho}}{2}\right|}\frac{e^2}{\left|\vec{R}+\frac{\vec{\rho}}{2}\right|}, \quad (1b)$$

depending on whether the process channel is an H scattering or a Ps formation one. $\vec{r}_1$ is the position vector of the positron, and $\vec{r}_2$ is that of the target electron. $\vec{\rho}=\vec{r}_1-\vec{r}_2$ and $\vec{R}=(\vec{r}_1+\vec{r}_2)/2$.

Let $\Psi_L(1,2)$ be the trial wave function of the collision system, corresponding to a total angular momentum L and a parity π. This wave function is formulated in the LS-coupling scheme. As usual, $\Psi_L(1,2)$ is expanded in terms of the target wave functions as

$$\Psi_L(1,2)=\sum_{n_p l_1 l_2} u_{n_p l_1}(r_1)F_{n_p l_1 l_2}(r_2)Y_{L l_1 l_2}^{M_L}(\hat{\mathbf{r}}\cdot\hat{\mathbf{r}}_2)+\sum_{n_q l_3 l_4}\phi_{n_q l_3}G_{n_4 l_3 l_4}(R)Y_{L l_3 l_3}^{M_L}(\hat{\boldsymbol{\rho}}\cdot\hat{\mathbf{R}}) . \quad (2)$$

We shall use $p=(n_p l_1 l_2)$ and $q=(n_q l_3 l_4)$ to indicate respectively a hydrogen scattering channel and a positronium formation channel. n_p, l_1, and l_2 are respectively the principal quantum number, orbital angular momentum of H, and orbital angular momentum of the scattered positron, while n_q, l_3, and l_4 are respectively the principal quantum number, intrinsic orbital angular momentum of Ps, and orbital angular momentum of Ps referred to the proton of H. A primary part of the method is to construct scattered (trial) wave functions for the hydrogen and positronium formation channels. These scattered waves are composed of two parts: a free part and a bound part. These scattered waves are explicitly written as

$$F_p(r_2)=\alpha_{0p}S_p(r_2)+\alpha_{1p}C_p(r_2)+\Omega_p(r_2) \quad (3a)$$

and

$$G_q(R)=a_{0q}S_q(R)+\alpha_{1q}C_q(R)+\Omega_q(R) , \quad (3b)$$

where the indices 0 and 1 correspond respectively to an S or to a C function. The independent free wave functions S and C are

$$S_p=k_p j_{l_2}(k_p r_2) , \quad (4a)$$

$$C_p(r_2)=k_p(1-e^{-\beta r_2})^{2l_2+1}n_{l_2}(k_p r_2) , \quad (4b)$$

$$S_q(R)=\sqrt{2}k_q j_{l_4}(k_q R) , \quad (4c)$$

$$C_q(R)=\sqrt{2}k_q(1-e^{-\gamma R})^{2l_4+1}n_{l_4}(k_q R) . \quad (4d)$$

It should be noted that shielding factors have been, as usual, introduced to force the spherical Newmann functions to behave correctly in terms of r_2 and R near the coordinate origin. These shielding factors are expressed in terms of the "stability parameters" β and γ.

The bound parts $\Omega_p(r_2)$ and $\Omega_q(R)$ are also expanded in terms of a numerable set of normalized basis functions $\eta_{p,i}(r_2)$ or $\eta_{q,j}(R)$,

$$\Omega_p(r_2)=\sum_i c_{p,i}\eta_{p,i}(r_2)\ , \tag{5a}$$

$$\Omega_q(R)=\sum_j c_{q,j}\eta_{q,j}(R)\ . \tag{5b}$$

$\Omega_p(r_2)$ and $\Omega_q(R)$ can also themselves be normalized. However, in practical calculations of a cross section, the normalization of these bound parts do not affect the results of the calculation.

The Harris-Nesbet procedure requires (as any method using variational techniques) that $(H-E)\Psi_L(1,2)$ has no component in the subspace of state vectors spanned by the short-range bound functions. This condition provides a "linkage" between the internal and external parts of the scattered waves, namely, the possibility for expressing the expansion coefficients of the bound parts in terms of those of the external parts.

By applying the Kohn variational method, Nesbet proved that the stationary reactance matrix is expressed in terms of the M matrix according to

$$R^{\mu\mu'}=-2\left[M_{00}^{\mu\mu'}+\sum_s \gamma_{\mu s}M_{10}^{s\mu'}\right]\Big/(k_\mu k_{\mu'})^{1/2}\ . \tag{6}$$

The M matrix is defined (by consequence of the "linkage") in terms of the so-called free-free N matrix and bound-free B matrices [15–17] of the processes

$$M_{ij}^{\mu\mu'}=N_{ij}^{\mu\mu'}+\sum_\alpha B_{i\alpha}^{\mu}(E-E_\alpha)^{-1}B_{\alpha j}^{\mu'}\ . \tag{7}$$

$\gamma_{\mu s}$ is a solution of the inhomogeneous system of linear equations

$$\sum_s M_{11}^{\mu' s}\gamma_{\mu s}=-M_{10}^{\mu'\mu}\ . \tag{8}$$

In M- and N-matrix elements, i and j (equal to 0 or 1) indicate an element corresponding either to a spherical Bessel or a spherical Newmann free channel, while $\mu=p,q$ and $\mu'=p',q'$ denote different (hydrogen or positronium) scattering channels. However, bound-free matrix elements such as $B_{i\alpha}^{\mu}$ connect an eigenstate α of the set of independent bound basis functions to a free state (either spherical Bessel or spherical Newmann function). Nesbet also proved that if the inverse Kohn variational method is considered, then the inverse reactance matrix will be expressed in terms of the M matrix according to

$$R_{\mu\mu'}^{-1}=2\left[M_{11}^{\mu\mu'}+\sum_s M_{01}^{s\mu'}\beta_{\mu s}\right]\Big/(k_\mu k_{\mu'})^{1/2}\ , \tag{9}$$

where $\beta_{\mu s}$ are solutions of the system of linear equations

$$\sum_s M_{00}^{\mu' s}\beta_{\mu s}=-M_{01}^{\mu'\mu}\ . \tag{10}$$

Once the R matrix was determined, the corresponding cross sections can then be evaluated according to the usual formula that relates the transition matrix with the reactance matrix.

II. NUMERICAL METHOD

In this calculation, the normalized basis functions that we used to expand the bound part of the scattered wave are of a Slater type. The exponents Z_v of these basis functions were chosen over a wide range of values to secure the convergence of the results of the calculation. The calculation was done with both Kohn and inverse Kohn methods for a mutual verification of the results. Essentially, we needed to analytically reduce elements of the bound-bound, overlapping, bound-free and free-free matrices [15–17] to forms that can be calculated by numerical computations. For matrix elements where both "in" and "out" channels are either hydrogen channels or positronium channels, we can obtain closed-form expressions. Their numerical computation can thereby be done quite easily and fast. However, matrix elements that involve both hydrogen and positronium channels can only be analytically reduced to two-variable integrals. As was pointed out above, the matrix elements in this latter case contain two different sets of coordinates ($\vec{r}_1,\vec{r}_2$, and $\vec{R},\vec{\rho}$). In order to reduce these formulas to two-variable integrals, we had to use the spheroidal coordinates, $\xi=(r_1+\rho)/r_2$ and $\eta=(r_1-\rho)/r_2$, and φ, which is an angle between the e^+e^-p plane an arbitrary plane running through the line e^+p. The double integrals were then evaluated with numerical quadrature. The analytical reduction of these matrix elements to either closed forms or two-variable integral forms were tedious and time consuming. Every effort had been made to ensure that the reduced formulas we obtained were absolutely free from error.

Depending on the number of basis functions used to expand the bound part of the trial function, the number of independent matrix elements that we needed to compute could be very great. For example, the number of independent bound-bound matrix elements for the six-state coupling scheme alone could be more than 60 000. Out of these, about one fourth of them required double quadrature to evaluate. Furthermore, the computation of some of these matrix elements for higher partial-wave L was difficult. As a result, the Harris-Nesbet calculation for positron scattering consumed a large amount of computer time.

The analytical formulas derived for these matrix elements and their numerical evaluation had also been double-checked by a comparison of the values, calculated with two completely different formulas that were independently obtained for these *symmetric* matrix elements. We were, therefore, confident that our analytical formulas obtained for these matrix elements should be free from error.

In general, our results of phase shifts (below the positronium formation threshold) and of cross sections (above the Ps formation threshold) calculated in the Kohn and inverse Kohn methods agreed with each other to four figures of significance at least. We also increased the number of bound basis functions until the results of cross section and phase shift did not change significantly. The stability of the results of calculation was also checked, employing the Schwartz's principle, by tentatively vary-

ing the values of the stability parameters. We believe that our numerical phase shifts had an accuracy better than 0.5% for partial-wave cross sections with L less than 4. For higher partial waves, we estimated that this accuracy might be a bit lower, but might not exceed 1% or, at worse, 2%. However, the values of these higher partial-wave cross sections are at least two orders of magnitude smaller than those of lower partial waves, and the 1% accuracy of these higher partial-wave cross sections would result in an inaccuracy of less than 0.01% for the integrated cross section as a whole. We were therefore content with the accuracy tolerance that we attained for the cross sections of $L=4$, 5, and 6 partial waves.

III. RESULTS AND DISCUSSION

A. Below the Ps formation threshold

We obtained the phase shifts and elastic cross sections at energies below the Ps formation threshold for the coupling schemes $(1s,2s)$H-$(1s,2s)$Ps, $(1s,2s,2p)$H-$(1s,2s)$Ps, and $(1s,2s,2p)$H-$(1s,2s,2p)$Ps. In Table I, we show the S-, P-, D-, F-, and G-wave phase shifts that we calculated with the Harris-Nesbet method, using these various coupling schemes. For the six-state [$(1s,2s,2p)$H-$(1s,2s,2p)$Ps] coupling scheme, our phase-shift values were found to agree very well with the ones calculated by Mitroy [7,8], who employed a completely different numerical method. This excellent agreement could imply two things. First, the Harris-Nesbet method did seem to be able to provide reliable results for large coupling schemes, as well as for higher partial-wave scatterings. Second, the calculation by Mitroy seemed to produce fairly accurate results for the phase shifts. Indeed, previous results of S- and P-wave phase shifts calculated by Mitroy [7] with the $(1s,2s,2p)$H-$1s$Ps coupling scheme seemed to also agree excellently with our previously calculated Harris-Nesbet values [12,13]. We quote these sets of phase-shift values in Table I for comparison. Also shown are the S-wave phase shifts calculated by Wakid and Labahn [17], who employed the same Harris-Nesbet method as we did. We believe that our S-wave phase shifts for the $(1s,2s,2p)$H-$(1s,2s,2p)$Ps scheme are slightly more accurate, since our values agreed better with those calculated by Mitroy [7] and since we considered for our calculation a number of basis functions greater than the one that Wakid and Labahn [17] had considered for their calculation. The agreement between our six-state S-, P-, and D-wave phases shifts and those of Sarkar and Ghosh [11] are only fair or poor. At some energy points, the discrepancy between our values and theirs is significant. For example, we quote their S-wave phase shifts in Table I.

For all cases, we noticed that the phase shifts were smaller in size for higher ($L>3$) partial-wave scatterings. Also, the difference between the phase shifts obtained with the coupling schemes $(1s,2s,2p)$H-$(1s,2s)$Ps and $(1s,2s)$H-$(1s,2s)$Ps were quite significant. This seemed to indicate that the polarization effect, included through the $2p$ state of hydrogen, influenced significantly the scattering of positron at low energies. However, the influence of the $2p$ Ps state on the phase shifts seemed to be much less dramatic. This was reflected in a smaller difference between the phase shifts calculated with the $(1s,2s,2p)$H-$(1s,2s,2p)$Ps and $(1s,2s,2p)$H-$(1s,2s)$Ps coupling schemes.

We also showed in Table I the S- and P-wave phase shifts calculated with a variational method by Bhatia *et al.* [22] to be compared with our close-coupling results. Assuming that these variational values are used as a yardstick for coupled-state calculations, the agreement of the six-state close-coupling values is expected not to be good, since the number of states (or pseudostates) that we included in the coupling scheme here may have not yet been sufficiently high to take care of all of the scattering effects, especially the one of the continuum polarization. It may be worthwhile to attempt a "large" coupled-state calculation with the Harris-Nesbet method.

To see how closely our six-state high-L phase shifts follow the approximate modified effective range theory (MERT) formula by O'Malley, Rosenberg, and Spruch [23] at low energies, we compared these $L=5$ and $L=6$ phase shifts in Fig. 1. Note that the approximate MERT formula is useful for high partial-wave scatterings when the "exact" numerical calculation becomes too involved. It was also very useful when the state-of-the-art of electronic computation was still not so good. Since the $2p$ physical state represents only about two thirds of the dipole polarizability [24] of the ground-state hydrogen, the polarizability used for the MERT formula in this case should be about 2.96 a.u. (a_0^3). It may be worth noting that here the Ps($2p$) state also makes some contribution to the effective dipole polarizability and may, therefore, modify this value somewhat. We used this value ($2.96a_0^3$) for the dipole polarizability in the MERT formula of $L>0$ to calculate the phase shifts. We found that the MERT formula provides $L=5$ and $L=6$ phase shifts, agreeing well at low energies with those we calculated with the Harris-Nesbet method (see Fig. 1). As expected, the agreement tends to worsen at higher energies. We also considered the $L=0$ MERT formula to the $O(k^3)$ to estimate the scattering length A_0 of the collision system when the six-state [$(1s,2s,2p)$H-$(1s,2s,2p)$Ps] scheme is employed. We found that $A_0=-0.874\,78$ a.u. The negative value obtained for the scattering length is as expected. It implies that the attractive long-range polarization potential alone in positron scattering does not gain a sufficient strength to produce S-wave bound states for the hydrogen-e^+ system.

The elastic cross sections below the positronium formation cross sections shown in Fig. 2 reconfirmed the remarks we made above about the phase shifts. Among these partial-wave cross sections, the S- and P-wave ones exhibit some distinct behavior. As usual, the Ramsauer-Townsend effect can be clearly seen in the S-wave cross section at an energy around 1.2 eV. The P-wave cross sections increase to a maximum and then gradually decrease as the positron energy increases. As the energy crosses the Ps threshold, the P-wave cross sections exhibit a visible bump just above the Ps formation threshold. We shall discuss this bump in more detail below. All the other partial-wave cross sections ($L=2$, 3, 4, 5, and 6; some of these were not shown) increase gradually as the

TABLE I. Partial-wave phase shifts (in radians) of positron-hydrogen scattering at energies below the positronium formation threshold. (a1) Wakid and Labahn [17] with coupling scheme $(1s,2s,2p)$H-$(1s)$Ps; (a2) Mitroy [7] with coupling scheme $(1s,2s,2p)$H-$1s$Ps; (a3) Harris-Nesbet algebraic calculation [12] with coupling scheme $(1s,2s,2p)$H-$1s$Ps; (b3) present Harris-Nesbet algebraic calculation with coupling scheme $(1s,2s)$H-$(1s,2s)$Ps; (c) present Harris-Nesbet calculation with coupling scheme $(1s,2s,2p)$H-$(1s,2s)$Ps; (d1) Wakid and Labahn [17] with coupling scheme $(1s,2s,2p)$H-$(1s,2s,2p)$Ps; (d2) Mitroy [7] with coupling scheme $(1s,2s,2p)$H-$(1s,2s,2p)$Ps; (d3) present Harris-Nesbet algebraic calculation with coupling scheme $(1s,2s,2p)$H-$(1s,2s,2p)$Ps; (d4) Sarkar and Ghosh [11] with coupling scheme $(1s,2s,2p)$H-$(1s,2s,2p)$Ps; (f) variational calculation by Bhatia *et al.* [22]. Numbers in brackets denote powers of 10 by which the preceding number is to be multiplied.

Scheme \ Momentum k (a.u.)	0.1	0.2	0.3	0.4	0.5	0.6	0.7
			S wave				
(a1)	0.0324	0.020 4	0.018 9	−0.0696	−0.1259	−0.1831	−0.2362
(a2)	0.0328	0.021 2	−0.016 4	−0.0672	−0.1231	−0.1796	−0.2324
(a3)	0.0331	0.021 3	−0.016 3	−0.0672	−0.1235	−0.1799	−0.2328
(b3)	0.0160	0.014 0	−0.011 8	−0.0567	−0.1120	−0.1698	−0.2248
(c)	0.0508	0.042 0	0.000 9	−0.0524	−0.1095	−0.1665	−0.2206
(d1)	0.0491	0.032 1	0.005 5	−0.0500	−0.1150	−0.1773	−0.2260
(d2)	0.0526	0.0451	0.005 53	−0.0472	−0.1041	−0.1607	−0.2138
(d3)	0.0525	0.045 06	0.005 54	−0.0473	−0.1044	−0.1609	−0.2141
(d4)	0.0530	0.045 7	0.004 49	−0.0492	−0.1035	−0.1605	−0.2146
(f)	0.1483	0.187 7	0.167 7	0.1201	0.0624	0.0039	−0.0512
			P wave				
(a2)	0.005 33	0.018 2	0.0342	0.0496	0.0615	0.0690	0.0770
(a3)	0.005 32	0.018 2	0.0342	0.0495	0.0613	0.0688	0.0768
(b3)	0.001 30	0.008 63	0.0221	0.0371	0.0487	0.0553	0.0618
(c)	0.005 43	0.018 6	0.0348	0.0506	0.0632	0.0717	0.0803
(d2)	0.006 27	0.022 2	0.0402	0.0558	0.0679	0.0759	0.0856
(d3)	0.006 24	0.022 1	0.0401	0.0558	0.0676	0.0758	0.0853
(f)	0.009	0.032 5	0.0659	0.1010	0.1303	0.1541	0.1792
			D wave				
(b3)	0.167[−4]	0.398[−3]	0.215[−2]	0.633[−2]	0.134[−1]	0.233[−1]	0.378[−1]
(c)	0.888[−3]	0.354[−2]	0.803[−2]	0.145[−1]	0.230[−1]	0.340[−1]	0.494[−1]
(d2)	0.904[−3]	0.375[−2]	0.848[−2]	0.151[−1]	0.238[−1]	0.352[−1]	0.519[−1]
(d3)	0.903[−3]	0.372[−2]	0.845[−2]	0.150[−1]	0.236[−1]	0.350[−1]	0.517[−1]
			F wave				
(d2)	0.296[−3]	0.122[−2]	0.278[−2]	0.502[−2]	0.809[−2]	0.124[−1]	0.191[−1]
(d3)	0.292[−3]	0.119[−2]	0.275[−2]	0.497[−2]	0.799[−2]	0.123[−1]	0.189[−1]
			G wave				
(d2)	0.130[−3]	0.542[−3]	0.123[−2]	0.222[−2]	0.351[−2]	0.524[−2]	0.772[−2]
(d3)	0.131[−3]	0.526[−3]	0.120[−2]	0.217[−2]	0.342[−2]	0.514[−2]	0.755[−2]

positron energy increases. The most significant contributions to the integrated cross sections some from *S*-, *P*-, and *D*-wave scatterings. A somewhat less significant contribution comes from *F*-wave (and probably *G*-wave) scattering. Contributions from $L=5$ and $L=6$ partial-wave scatterings to the integrated cross sections are almost negligible at these low energies. For this reason, we only calculated the partial cross sections up to $L=6$ to be summed for the integrated cross sections. The integrated elastic cross sections at energies below the positronium formation threshold are shown in Fig. 6 for the $(1s,2s,2p)$H-$(1s,2s,2p)$Ps coupling scheme. It shows the Ramsauer-Townsend effect at a very low energy around 1.2 eV. In particular, the integrated cross sections for the six-state coupling scheme (Fig. 6) seemed to agree very well with those shown in Mitroy and Stelbovics's publication[8].

B. Above positronium formation threshold

In Tables II and III, we tabulate elastic cross sections and Ps formation cross sections for *S*-, *P*-, and *D*-wave scatterings for a number of energy points. These cross sections were calculated with the $(1s,2s)$H-$(1s,2s)$Ps, $(1s,2s,2p)$H-$(1s,2s)$Ps, and $(1s,2s,2p)$H-$(1s,2s,2p)$Ps coupling schemes. We also show the so-called integrated cross sections for elastic scattering and positronium formation processes. Values of cross sections were obtained at several energy points in the Ore gap for seven first partial waves $L=0$, 1, 2, 3, 4, 5, and 6. The integrated cross

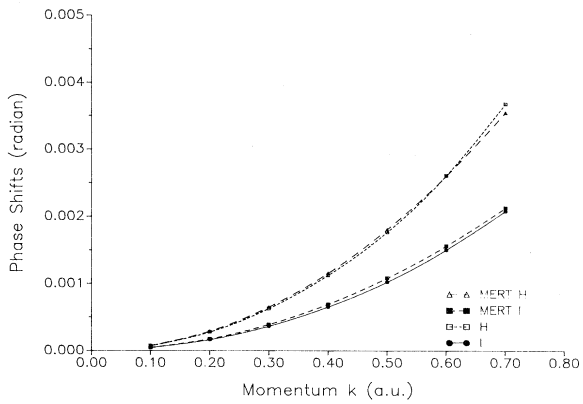

FIG. 1. Comparison between phase shifts (in radians) calculated by the Harris-Nesbet method with the $(1s,2s,2p)$H-$(1s,2s,2p)$Ps coupling scheme and those calculated by the MERT formula [23] for $L=5$ and $L=6$ partial waves.

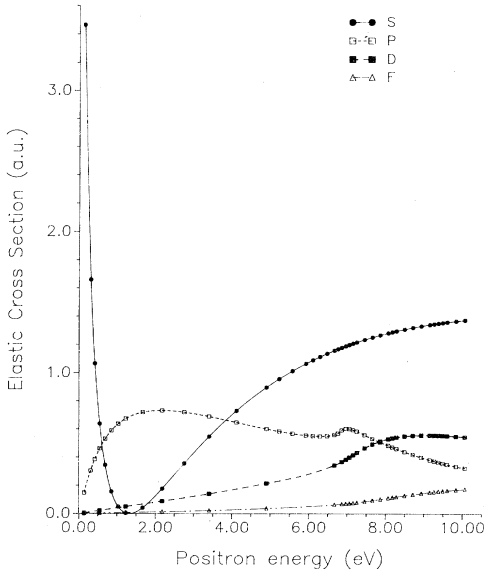

FIG. 2. S-wave elastic cross sections in atomic units for positron-hydrogen scattering. S, S wave; P, P wave; D, D wave; F, F wave.

sections were estimated by adding these seven partial cross sections together. The contribution from partial cross sections with L higher than 6 is very small, and their contribution, if counted, is expected to not alter the integrated cross sections significantly. For example, the values of the $L=5$ and $L=6$ Ps formation cross sections at $k=0.71$ a.u. were extremely small. Thus, neglecting these higher partial-wave cross sections (with L greater than 6) is not expected to alter the integrated cross sections by more than 5%.

We also included in Tables II and III the elastic and positronium formation cross sections calculated with a variational method by Humberston and Brown [5,6] for

TABLE II. Elastic cross sections (in πa_0^2) for positron-hydrogen scattering at energies in the Ore gap. Same as in Table I, except that (f) is a variational calculation [5,6]. Numbers in brackets denote powers of 10 by which the preceding number is to be multiplied.

Scheme \ Energy (Ry) of positron	0.5041	0.525 625	0.5625	0.600 625	0.6400	0.680 625	0.7225
			S wave				
(a3)	0.439	0.449	0.462	0.472	0.481	0.488	0.492
(b3)	0.412	0.422	0.436	0.448	0.458	0.466	0.472
(c)	0.397	0.407	0.421	0.433	0.443	0.451	0.457
(d2)	0.374		0.397		0.419		0.434
(d3)	0.375	0.384	0.398	0.410	0.420	0.428	0.435
(f)	0.26[−1]		0.43[−1]		0.65[−1]		0.85[−1]
			P wave				
(a3)		0.155	0.141	0.124	0.108	0.947[−1]	0.831[−1]
(b3)	0.984[−1]	0.101	0.942[−1]	0.838[−1]	0.736[−1]	0.644[−1]	0.565[−1]
(c)	0.165	0.168	0.153	0.136	0.121	0.107	0.958[−1]
(d2)	0.189		0.170		0.134		0.107
(d3)	0.188	0.189	0.169	0.150	0.133	0.118	0.106
(f)	0.789		0.724		0.622		0.547
			D wave				
(a3)	0.929[−1]	0.104	0.122	0.134	0.140	0.142	0.141
(b3)	0.635[−1]	0.735[−1]	0.907[−1]	0.104	0.113	0.115	0.121
(c)	0.106	0.119	0.141	0.155	0.161	0.162	0.160
(d2)	0.118		0.158		0.178		0.176
(d3)	0.117	0.132	0.157	0.171	0.177	0.177	0.175
(f)	0.323		0.403		0.423		0.413
			Integrated				
(b3)	0.581	0.604	0.632	0.651	0.664	0.673	0.678
(d2)	0.710		0.763		0.786		0.787
(d3)	0.708	0.736	0.761	0.776	0.784	0.785	0.784

TABLE III. Positronium formation cross sections (in πa_0^2) for positron-hydrogen scattering at energies in the Ore gap. Same as in Table I, except that (d1) is now Hewitt, Noble, and Bransden [9]; (d4) is Sarkar and Ghosh [11]; and (f) is a variational calculation [5,6]. Numbers in brackets denote powers of 10 by which the preceding number is to be multiplied.

Scheme \ Energy (Ry) of positron	0.5041	0.525 625	0.5625	0.600 625	0.6400	0.680 625	0.7225
			S wave				
(a2)	0.253[−2]		0.407[−2]		0.277[−3]		0.143[−3]
(a3)	0.254[−2]	0.428[−2]	0.411[−2]	0.343[−2]	0.271[−2]	0.203[−2]	0.144[−2]
(b2)	0.58[−3]		0.256[−2]		0.389[−2]		0.404[−2]
(b3)	0.582[−3]	0.154[−3]	0.257[−2]	0.331[−2]	0.380[−2]	0.403[−2]	0.404[−2]
(c)	0.101[−2]	0.164[−2]	0.163[−2]	0.146[−2]	0.126[−2]	0.105[−2]	0.844[−3]
(d1)			0.49[−2]		0.64[−2]		0.12[−2]
(d2)	0.181[−3]		0.154[−4]		0.538[−4]		0.886[−4]
(d3)	0.181[−3]	0.103[−3]	0.963[−5]	0.593[−5]	0.417[−4]	0.790[−4]	0.964[−4]
(d4)			0.30[−3]		0.84[−4]		0.40[−4]
(f)	0.41[−2]		0.44[−2]		0.49[−2]		0.58[−2]
			P wave				
(a2)	0.115[−1]		0.276		0.412		0.470
(a3)		0.129	0.278	0.361	0.411	0.445	0.470
(b3)	0.988[−2]	0.105	0.238	0.322	0.377	0.415	0.441
(c)	0.112[−1]	0.126	0.265	0.340	0.388	0.424	0.455
(d1)			1.47		0.259		1.44
(d2)	0.172[−1]		0.294		0.406		0.460
(d3)	0.173[−1]	0.161	0.295	0.362	0.404	0.434	0.459
(d4)			0.279		0.380		0.445
(f)	0.27[−1]		0.365		0.482		0.561
			D wave				
(a2)	0.289[−3]		0.145		0.465		0.687
(a3)	0.289[−3]	0.229[−1]	0.144	0.309	0.464	0.590	0.685
(b3)	0.310[−3]	0.236[−1]	0.142	0.304	0.462	0.599	0.712
(c)	0.321[−3]	0.257[−1]	0.163	0.348	0.516	0.650	0.749
(d1)			0.570		0.933		0.771
(d2)	0.435[−3]		0.199		0.576		0.809
(d3)	0.436[−3]	0.344[−1]	0.199	0.400	0.575	0.710	0.809
(d4)			0.192		0.558		0.790
(f)	0.62[−3]		0.335		0.812		1.057
			Integrated				
(b3)	0.108[−1]	0.132	0.401	0.700	1.00	1.29	1.56
(d2)	0.179[−1]		0.5194		1.201		1.812
(d3)	0.179[−1]	0.197	0.521	0.861	1.20	1.52	1.81

comparison. As was pointed out above, the agreement of the six-state close-coupling results with the variational values is not expected to be good. The agreement between the positronium formation cross sections seems somewhat better.

It can be seen in Table III that our *S*, *P*, and *D* partial-wave cross sections for positronium formation that we calculated with the six-state [$(1s,2s,2p)$H-$(1s,2s,2p)$Ps] coupling scheme agreed very well with those calculated by Mitroy [7,8], but completely disagreed with those calculated by Hewitt, Noble, and Bransden [9]. It should be stressed again that the reliability of our algebraic results was safeguarded by many self-consistency checks that are provided by the Harris-Nesbet method. The discrepancy between the two sets of results at some energy points, taking under consideration the round-off effect, was estimated to be, at worst, less than 0.5%. We believe that this slight discrepancy could be narrowed down further by improving the accuracy of both calculations.

We note that the cross sections that were also calculated by the Durham group but for the $(1s,2s,2p)$H-$1s$Ps coupling scheme [9] are in fair agreement with our Harris-Nesbet ones and hence, they also agree fairly well with those calculated by Mitroy. This slight difference might arise from the fact that the Durham group used the Gaussian-type basis functions for their calculation, while Mitroy and Stelbovics, presumably, used the exact hydrogen wave functions. The fair agreement for this coupling scheme implies that the serious disagreement found for the results of the Durham group in the $(1s,2s,2p)$H-$(1s,2s,2p)$Ps coupling scheme might originate from their calculation of the transition matrix elements between the $1s$, $2s$, and $2p$ positronium states. This point was also mentioned by Mitroy [7,8]. The agreement between our Ps formation cross sections and those of Sarkar and Ghosh [11] is also very poor. In particular,

the S-wave values of this group differ considerably from ours and Mitroy's [7].

Only a minor discrepancy between our results and those calculated by Mitroy [7] was detected for the S-wave positronium formation cross sections at $E=0.5625$, $E=0.64$, and $E=0.7225$ Ry, but this slight discrepancy should not be of any concern, since these values of S-wave cross sections were very small [of the order of $1.00(-4)$]. In spite of this smallness, we believe that this unimportant discrepancy may be resolved by improving the accuracy of both calculations further. Our S-wave Ps formation cross sections for the coupling scheme $(1s,2s)$H-$(1s,2s)$Ps also agreed well with those calculated by Mitroy [7].

The elastic cross sections for partial waves above $L=3$ increased gradually in this energy region of the Ore gap. The D-wave cross sections also increased gradually but began to drop slightly at the top end of the Ore gap. The elastic cross sections above the positronium formation threshold are shown in more detail in Fig. 2 for S-, P-, D-, and F-wave scatterings.

A feature which might be worth noting was seen near the positronium formation threshold in the elastic cross sections for P-wave scattering (Fig. 3). There was a clear bump just above the positronium formation threshold. After the elastic cross sections slightly dipped down, they immediately rose at energies just below the Ps threshold to form this bump through the Ps threshold. This bump occurred for all the three coupling schemes considered here. The bump was more enhanced for a coupling scheme that contains a strong polarization effect, through the presence of the $2pH$ and $2pPs$ states in the coupling scheme. Thus, its existence might be enhanced by the long-range polarization potential. However, the dynamical origin of the formation of this P-wave bump remains unclear. It was also seen in Higgins and Burke's calculation [10] and for other coupling schemes [12,25]. The P-wave bump left a slight but visible trace at this energy region in the integrated elastic cross sections (see Fig. 6).

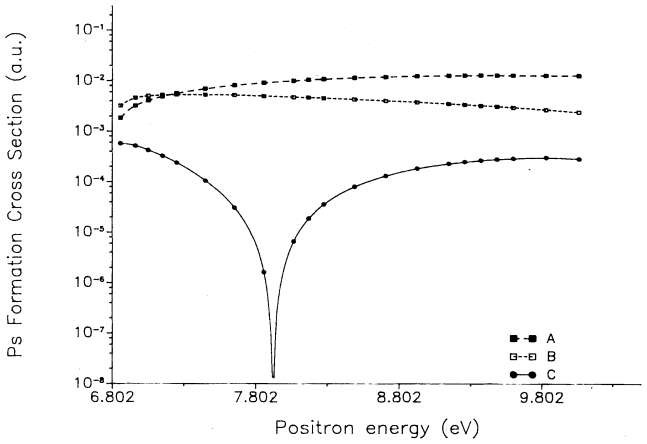

FIG. 4. Ps formation cross sections in atomic units for positron-hydrogen scattering. A, $(1s,2s)$H-$(1s,2s)$Ps coupling scheme; B, $(1s,2s,2p)$H-$(1s,2s)$Ps coupling scheme; C, $(1s,2s,2p)$H-$(1s,2s,2p)$Ps coupling scheme.

This trace was also visible in the integrated and partial cross sections of Mitroy and Stelbovics [8], using the same six-state coupling scheme. Our integrated elastic cross sections for the six-state coupling scheme in the Ore gap shown in Fig. 6 also agreed very well with those calculated by Mitroy and Stelbovics [8].

The positronium formation cross sections in the Ore gap are shown in Figs. 4 and 5 for S-, P-, D-, and F-wave scattering. Except for the case of S-wave scattering, for all other cases, including the G-, H-, and I-wave ones (not shown), the Ps formation cross sections increase as the positron energy increases from the Ps formation threshold to the upper end of the Ore gap (~ 10.10 eV). The P-wave cross sections and, to a lesser extent, the D-wave cross sections flatten out at the top end of the Ore gap. The only exception is the S-wave positronium formation cross sections calculated with the six-state coupling

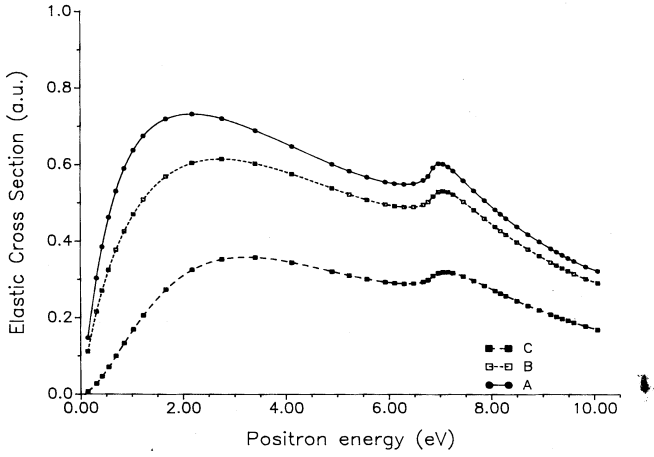

FIG. 3. P-wave elastic cross sections in atomic units for positron-hydrogen scattering. A, $(1s,2s,2p)$H-$(1s,2s,2p)$Ps coupling scheme; B, $(1s,2s,2p)$H-$(1s,2s)$Ps coupling scheme; C, $(1s,2s)$H-$(1s,2s)$Ps coupling scheme.

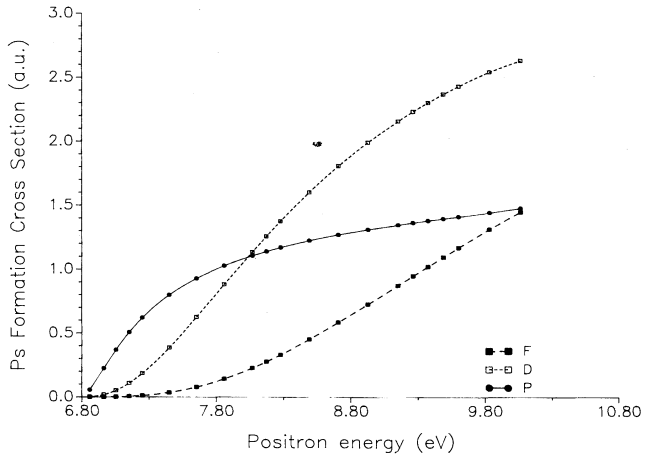

FIG. 5. Positronium formation cross sections in atomic units for positron-hydrogen scattering. P, P-wave; D, D wave; F, F wave.

schemes $(1s,2s,2p)$H-$(1s,2s,2p)$Ps. Here, similar to the results of the Ps formation cross section obtained in one of our previous calculations with the $(1s,2s,2\bar{p})$H-$1s$Ps coupling scheme [12], a dip was seen to form in this energy region (see Fig. 4). Offhand, we could not find a sound (dynamical) explanation for the formation of this dip in the S-wave positronium formation cross sections and especially for the fact that this dip was found to form only in the $(1s,2s,2p)$H-$(1s,2s,2p)$Ps coupling scheme but not in the other two. The positronium formation cross sections calculated with the two other coupling schemes [$(1s,2s,2p)$H-$(1s,2s)$Ps and $(1s,2s)$H-$(1s,2s)$Ps] tend to flatten out after a quick rise at the threshold. The dip seen in the case of the $(1s,2s,2p)$H-$(1s,2s,2p)$Ps coupling scheme did not, however, affect the integrated positronium formation cross sections significantly, since the S-wave positronium formation cross sections were very small in this region. The most significant contribution to the integrated positronium formation cross sections in this energy region comes from the P-, D-, and F-wave scattering. In Fig. 6, we exhibit the integrated positronium formation cross sections for the $(1s,2s,2p)$H-$(1s,2s,2p)$Ps coupling scheme. The integrated positronium formation cross sections increase linearly as the energy increases.

We also show in Fig. 6 the total (elastic plus positronium formation) cross sections for positron-hydrogen scattering at energies in the Ore gap. These cross sections were calculated with the six-state coupling scheme. We tentatively (and tentatively only) made a visual comparison with experimental values of cross section measured by the Detroit group [4] in this energy region. While there seemed to be a qualitative agreement in the shape of the cross sections, the theoretical and experimental cross sections did not seem to agree well with each other quantitatively. The discrepancy is as expected. Indeed, we did not expect that the coupling schemes we considered here had been sufficient to obtain "convergent" cross sections for a meaningful quantitative comparison. However, experiments of positron scattering from atomic hydrogen have been known to be difficult, and one should not, therefore, expect to have accurate results obtained right away for these early measurements. Besides, it has also been well known that in the Detroit experiment there was some difficulty with a discrimination against incident positrons going into small scattering angles, and this difficult may distort its results of cross section as well.

For completeness, we also show in Fig. 7 the S, P, D, and F waves and integrated cross sections for Ps$(1s)$-p elastic scattering. These cross sections were calculated with the six-state coupling scheme. In general, the cross sections for this process are much greater than the corresponding ones for elastic positron-hydrogen scattering. The elastic Ps$(1s)$-p cross sections exhibit many interesting features worth noting. The S-wave cross sections calculated with the $(1s,2s,2p)$H-$(1s,2s,2p)$Ps coupling scheme show the Ramsauer-Townsend effect at an energy below 0.25 eV. However, we found that this effect does not seem to remain visible for the $(1s,2s,2p)$H-$(1s,2s)$Ps and $(1s,2s)$H-$(1s,2s)$Ps coupling schemes. The P-wave cross sections of the six-state coupling scheme show a maximum peak near the zero-energy threshold, before they fall off quickly to zero. This P-wave Ps$(1s)$-p peak was found to totally disappear in the four-state coupling scheme case and to only leave a slight trace in the five-state coupling scheme case. For D-wave scattering, this peak becomes much broader and again, it can only be obviously seen in the six-state coupling scheme case. Since the $2p$ Ps state was present only in the six-state coupling scheme, the relatively strong long-range polarization potential that comes from this state may be responsible for

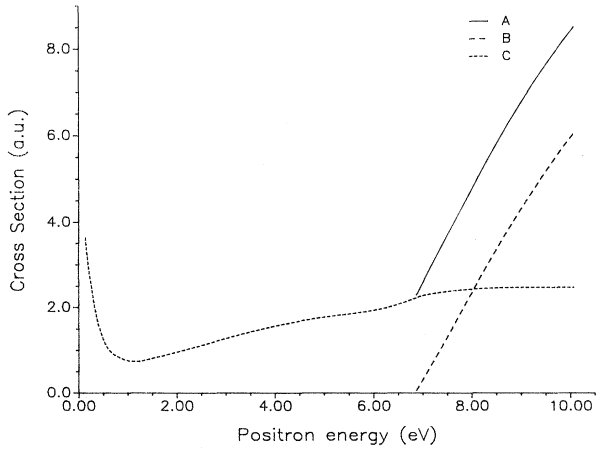

FIG. 6. Integrated and total cross sections in atomic units for positron-hydrogen scattering. A, total cross sections; B, Ps formation cross section; C, integrated elastic cross sections.

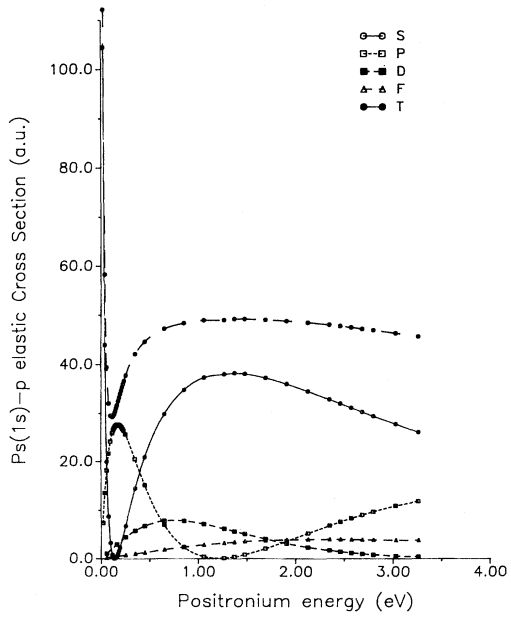

FIG. 7. Ps$(1s)$-p elastic cross sections in atomic units with the $(1s,2s,2p)$H-$(1s,2s,2p)$Ps coupling scheme. S, S-wave cross sections; P, P-wave cross sections; D, D-wave cross sections; F, F-wave cross sections; T, integrated cross sections.

these special features, especially for the Ramsauer-Townsend effect in the Ps($1s$)-p incoming channel. The integrated cross sections shown in this figure were again taken to be sums of the cross sections of the first seven partial-wave scatterings. The integrated cross sections for the six-state coupling scheme exhibit the Ramsauer-Townsend effect at a very small Ps energy. They then flatten out at energies in the Ore gap.

CONCLUSION

In this work, we employed the Harris-Nesbet method to carry out an extensive calculation of elastic and positronium formation cross sections with the six-state ($1s,2s,2p$)H-($1s,2s,2p$)Ps coupling scheme at low energies. We have succeeded in carrying out the calculation for high partial waves with coupling schemes of this type. Despite the complexity of this calculation, this work demonstrated that the Harris-Nesbet method can provide numerically reliable results for a more extended coupling scheme, as well as for high partial waves. Many interesting features were found for these results of cross section. These features may not disappear when a larger coupling scheme, including pseudostates, is considered for the calculation. The results of cross section presented here, which were obtained with a completely different numerical method, were also useful for a comparison with the close-coupling results obtained by solving the coupled Lippmann-Schwinger equations in momentum space. Our Harris-Nesbet calculation confirmed that one [7,8] of the three close-coupling results previously calculated by other groups for this coupling scheme is numerically accurate, while the other two [9,11] seem to be erroneous and/or inaccurate. Considering the fact that the algebraic method by Harris and Nesbet by itself has several self-consistency checks to safeguard the reliability and accuracy of the results obtained, the results of this method might also be used to double check the correctness of the results obtained by other methods of approximation. With the success gained in this work, we are contemplating the use of the Harris-Nesbet method to calculate cross sections in larger coupling schemes (including pseudostates and/or correlation functions), as well as to investigate Feshbach and shape resonances in positron collisions with hydrogen. We also plan to extend the range of scattering energy to higher energies. It may be worth noting that Mitroy, Berge, and Stelbovics recently [26] carried out some of these large calculations, using the method of solving the coupled Lippmann-Schwinger equations in momentum space.

ACKNOWLEDGMENT

This work was supported by the Natural Science and Engineering Research Council of Canada (NSERC).

[1] See, for example, Positron Interaction with Gases, Proceedings of the Positron Workshop [Hyperfine Inter. **73**, 1 (1992)].
[2] See, for example, M. Charlton and G. Laricchia, J. Phys. B **23**, 1045 (1990).
[3] W. Sperber, D. Becker, K. G. Lynn, W. Raith, A. Schwab, S. Sinapius, G. Spitcher, and M. Weber, Phys. Rev. Lett. **68**, 3690 (1992).
[4] S. Zhou, W. E. Kauppila, C. K. Kwan, and T. S. Stein, Phys. Rev. Lett. **72**, 1443 (1994).
[5] J. W. Humberston, J. Phys. B **17**, 2353 (1984).
[6] C. J. Brown and J. W. Humberston, J. Phys. B **18**, L401 (1995).
[7] J. Mitroy, Aust. J. Phys. **46**, 751 (1993); J. Phys. B **26**, 4861 (1993); **26**, L625 (1993).
[8] J. Mitroy and A. Stelbovics, J. Phys. B **27**, 3257 (1994).
[9] R. N. Hewitt, C. J. Noble, and B. H. Bransden, J. Phys. B **23**, 4185 (1990); **24**, L635 (1991).
[10] K. Higgins and P. G. Burke, J. Phys. B **26**, 4269 (1993).
[11] N. K. Sarkar and A. S. Ghosh, J. Phys. B **27**, 759 (1994).
[12] Guo Guang Liu and T. T. Gien, Phys. Rev. A **46**, 3918 (1992); **49**, 5157(E) (1994).
[13] T. T. Gien and Guo Guang Liu, Phys. Rev. A **48**, 3386 (1993).
[14] P. E. Harris, Phys. Rev. Lett. **19**, 173 (1967).
[15] R. K. Nesbet, Phys. Rev. **175**, 134 (1968); **179**, 60 (1969); *Variational Methods in Electron-Atom Scattering Theory* (Plenum, New York, 1980).
[16] G. J. Seiler, R. S. Oberoi, and J. Callaway, Phys. Rev. A **3**, 2006 (1971).
[17] S. E. A. Wakid and R. W. Labahn, Phys. Rev. A **6**, 2039 (1971).
[18] S. E. A. Wakid, Phys. Rev. A **8**, 2456 (1973).
[19] T. T. Gien, J. Phys. B **27**, L25 (1994).
[20] T. T. Gien and G. G. Liu, J. Phys. B **27**, L179 (1994).
[21] F. E. Harris and H. H. Michels, Phys. Rev. Lett. **22**, 1036 (1969); R. K. Nesbet and R. S. Oberoi, Phys. Rev. A **6**, 1885 (1972); R. K. Nesbet, *ibid.* **18**, 955 (1978).
[22] A. K. Bhatia, A. Temkin, R.J. Drachman, and H. Eiserike, Phys. Rev. A **3**, 1328 (1971); **9**, 219 (1974).
[23] T. F. O'Malley, L. Rosenberg, and L. Spruch, Phys. Rev. **125**, 1300 (1962).
[24] R. Damburg and E. Karule, Proc. Phys. Soc. London **90**, 637 (1967).
[25] T. T. Gien (unpublished).
[26] J. Mitroy, L. Berge, and A. Stelbovics, Phys. Rev. Lett. **73**, 2966 (1994).